Simulation Modeling of an Enhanced Low-Emission Swirl-Cascade Burner

FINAL TECHNICAL REPORT

10/01/2002 through 6/30/2004

Dr. Ala Qubbaj, Mechanical Engineering Department

September 2004

DE-FG2602NT41682

University of Texas pan American
1201 West University Drive
Edinburg, Texas 78539-2999

DISCLAIMER NOTICE

This report was prepared as an account of work sponsored by an agency of the United States Government. Neither the United States Government nor any agency thereof, or any of their employees, makes any warranty, express or implied, or assumes any legal liability or responsibility of the accuracy, completeness, or usefulness of any information, apparatus, product, or process disclosed, or represents that its use would not infringe privately owned rights. Reference herein to any specific commercial product, process, or service by trade name, trademark, manufacturer, or otherwise does not necessarily constitute or imply its endorsement, recommendation, or favoring by the United States Government or ant agency thereof. The views and opinions of authors expressed herein do not necessarily states or reflect those of the United States Government or ant agency thereof.

ABSTRACT

"Cascade-burners" is a passive technique to control the stoichiometry of the flame through changing the flow dynamics and rates of mixing in the combustion zone with a set of venturis surrounding the flame. Cascade-burners have shown advantages over other techniques; its reliability, flexibility, safety, and cost makes it more attractive and desirable. On the other hand, the application of "Swirl-burners" has shown superiority in producing a stable flame under a variety of operating conditions and fuel types. The basic idea is to impart swirl to the air or fuel stream, or both. This not only helps to stabilize the flame but also enhances mixing in the combustion zone. As a result, nonpremixed (diffusion) swirl burners have been increasingly used in industrial combustion systems such as gas turbines, boilers, and furnaces, due to their advantages of safety and stability. Despite the advantages of cascade and swirl burners, both are passive control techniques, which resulted in a moderate pollutant emissions reduction compared to SCR, SNCR and FGR (active) methods. The present investigation will study the prospects of combining both techniques in what to be named as "an enhanced swirl-cascade burner".

Natural gas jet diffusion flames in baseline, cascade, swirl, and swirl-cascade burners were numerically modeled using CFDRC package. The thermal, composition, and flow (velocity) fields were simulated. The numerical results showed that swirl and cascade burners have a more efficient fuel/air mixing, a shorter flame, and a lower NOx emission levels, compared to the baseline case. The results also revealed that the optimal configurations of the cascaded and swirling flames have not produced an improved performance when combined together in a "swirl-cascade burner". The non-linearity and complexity of the system accounts for such a result, and therefore, all possible combinations, i.e. swirl numbers (SN) versus venturi diameter ratios (D/d), need to be considered.

TABLE OF CONTENTS

A. INTRODUCTION

The primary objectives in burner design are to increase combustion efficiency and to minimize the formation of environmentally hazardous emissions such as nitrogen oxides (NO_x) and carbon monoxide (CO). Critical design factors that impact combustion include: the temperature and residence time of the combustion zone, the initial temperature of the combustion air, the amount of excess air and turbulence in the burner, and the manner in which the air and fuel streams are delivered and mixed. Elevated temperatures and excess air contribute to better burning of the fuel but lead to high levels of NO_x. Lower temperatures and fuel-rich mixtures produce incomplete (inefficient) combustion, which lead to elevated levels of CO. The design of a good burner thus involves finding an optimal balance between these conflicting requirements. In this respect, CFD can serve as a powerful tool.

Different technologies to control pollutant emissions from combustion systems (particularly NOx) have been developed. Flue Gas Recirculation (FGR), water injection, after burning, selective catalytic reduction (SCR), and non-catalytic reduction (SNCR), are active post combustion techniques that have been employed (Bowman[1], Gupta and Lilley [2]). On the other hand, passive techniques to manipulate the flow dynamics and rates of mixing of reactants in the combustion zone have been the focus of research in the last decade. The application of non-axisymmetric burner-exit geometries (Kamal and Gollahalli[3], Papanikolau and Wierzba[4], Papanikolau et al.[5]), staging of fuel-air mixing (Turns[6]), swirl burners (Tomeczek et al.[7], Cheng et al. [8]), as well as venturi-cascading (Qubbaj and Gollahalli[9,10]) are examples of such techniques.

"Venturi-cascading" technique was developed by Qubbaj and Gollahalli (Qubbaj and Gollahalli[9,10]). The basic idea behind this technique is controlling the stoichiometry of the flame through changing the flow dynamics and rates of mixing in the combustion zone with a set of venturis surrounding the flame. Venturi-cascading has shown advantages over other techniques; its reliability, flexibility, safety, and cost makes it more attractive and desirable. However, it has resulted in a moderate pollutant emissions reduction compared to SCR, SNCR and FGR methods.

Swirl combustion has shown superiority over other techniques as well; it meets a further important design objective of producing a stable flame under a variety of operating conditions and fuel types. The basic idea is to impart swirl to the air or fuel stream, or both.

This not only helps to stabilize the flame but also enhances mixing in the combustion zone. As a result, nonpremixed (diffusion) swirl burners have been increasingly used in industrial combustion systems such as gas turbines, boilers, and furnaces, due to their advantages of safety and stability, and consequently have a strong influence on flame emissions. Previous studies have reported significant improvements in the combustion and emission characteristics of combustion systems utilizing swirl flow configurations (Tomeczek et al.[7], Cheng et al. [8], Lyon[11], Tangirala et al.[12], Chen and Driscoll[13], Fric[14]). In many combustion devices both reactants are in gas phase and for technological reasons the coaxial geometry is commonly used to merge the two streams (Villermaux[15]); the swirl motion is used to improve flame stability and enhance mixing processes (Chen and Driscoll[13], Hillemans et al. [16]).

Despite the advantages of cascade and swirl burners, both are passive control techniques, which resulted in a moderate pollutant emissions reduction compared to SCR, SNCR and FGR (active) methods. The present investigation will study the prospects of combining both techniques in what to be named as "an enhanced swirl-cascade burner". In previous studies by the authors (Qubbaj and Gollahalli[9,10], Qubbaj et al.[17]), the optimal performance conditions for each of the cascade and swirl burners, in terms of swirl number (SN) and venturi diameter ratio (D/d), were deduced to be 1 and 1.25 respectively. In this study, the cascaded (D/d=1.25), swirling (SN=1), as well as the combined swirling-cascaded flames are numerically simulated.

The general goal of the current research is the improvement and optimization of the mixing processes between the reactants in such a way to minimize the environmental impact of combustion systems. Any improvement in the combustion performance relative to pollutant formation, stability, and overall efficiency requires a careful study of the flow field and mixing processes, particularly in such a highly turbulent reacting flow. The scaling of pollutant emissions in industrial flames is very difficult because of the complex geometry of the burner and the many parameters involved. The experimental evidence is that each burner is a unique device and even small geometry changes can influence the level of emissions. Earlier studies showed that swirl flows require a detailed flow structure and specification of the inlet conditions (Charles et al.[18], Starner and Bilger[19], Shen et al. [20]). The fluid dynamic analysis is very useful to provide the preliminary information about the mixing process.

Therefore, in this study, CFD simulations are used to simulate the flow, thermal, and composition fields in the primary mixing zone produced by venturi-cascading, air-swirling, as well as swirl-cascading in a turbulent non-premixed combustor.

B. PHYSICAL MODEL

Figure 1(a) shows the actual physical model, which consists mainly of a combustion chamber made from steel, 63.5 cm x 63.5 cm cross-section and 139.7 cm height. The chamber is provided with air-cooled Pyrex windows of dimensions 38.1 cm x 114.3 cm on all four sidewalls. The top of the chamber is connected to the atmosphere through an exhaust duct (as seen in Fig. 1). The fuel and oxidant are introduced to the combustion chamber through separate streams in a non-premixed or diffusion combustion process. The fuel is introduced through a stainless steel burner, of internal diameter 3.2 mm, inserted in the centerline of the chamber, and the air is introduced through an annular inlet of diameter 0.2 m, surrounding the fuel burner as depicted in Figure 1. Swirl is imparted to the air stream at swirl number (SN) of 1. The swirl number represents the ratio between the angular and axial air velocities. The cascade consists of a set of four identical venturis, with circular arc profiles, to form a cascade. The dimensions of the venturis are given in table 1 and shown in Fig. 1(a). The simplified physical model used in the computations, assuming axisymmetric flow conditions, is provided in Fig. 1(b). The operating and boundary conditions are given in Table 1.

Table 1: Operating and Boundary Conditions

Fuel	Natural Gas (95%+)
Burner diameter (d_b)	3.175 mm
Jet-exit Reynolds number	9000
Jet-exit/ Fuel axial velocity u_x	46.65 m/s
Venturi throat diameter (d)	0.0625 m
Venturi diameter ratio (D/d)*	1.25
Angular air velocities u_θ	3 m/s
Axial air velocity u_x	0.3 m/s
Swirl number (rw/U)	1.0
Near-burner axial location: x/d	4.63
Ambient temperature	295 K
Ambient pressure	100 kPa

*See Fig. 1(a)

C. NUMERICAL COMPUTATIONS

Computational Model

The numerical computations were conducted using the *CFDRC-ACE+*, advanced computational environment package 2002, in which CFD-GEOM (Interactive Geometric Modeling and Grid Generation software) and CFD-VIEW (3-D Computer Graphics and Animation Software) are incorporated. The computational domain encompassed half of the flame jet assuming axisymmetric flow conditions (as seen in Fig. 2) and extended to 139.7 cm in the axial direction and 31.75 cm in the radial direction. The grid cells were generated with increasing spacing in the radial and axial directions; this provided an adequate resolution where gradients were large, i.e., near the centerline, and saved CPU time where gradients were small, near the edges.

The venturis were modeled as two-dimensional axisymmetric convergent nozzles around the jet. With the cascade being added to the jet, the geometric complexity of the problem increased; which required multi-domain structured grid systems to be connected and matched on the boundaries. The CFD-GEOM module (Interactive Geometric Modeling and Grid Generation Software) in the CFD-ACE+ package was used for geometric modeling and grid generation purposes.

A cell-centered control volume approach was used, in which the discretized equations or the finite difference equations (FDE) were formulated by evaluating and integrating fluxes across the faces of control volumes in order to satisfy the Favre-averaged continuity, momentum, energy and mixture fractions conservation equations (Eqs. 1, 2, 4 and 9, respectively). The first order upwind scheme was used for evaluating convective fluxes over a control volume. The well-known SIMPLEC algorithm, proposed by Van Dooormal and Raithby[21], was used for velocity pressure-coupling. SIMPLEC stands for “Semi-Implicit Method for Pressure-Linked Equation Consistent”, in which an equation for pressure correction is derived from the continuity equation. The standard k-ε model was used to close the set of equations.

Governing Equations

The code CFD-ACE+ employs a conservative finite-volume methodology and accordingly all the governing equations are expressed in a conservative form in which tensor notation is generally employed. The basic governing equations are for the conservation of mass, momentum and energy:

Continuity equation:

$$\frac{\partial \rho}{\partial t} + \frac{\partial}{\partial x_j}(\rho u_j) = 0 \quad \text{.....(1)}$$

where u_j is the j^{th} Cartesian component of velocity and ρ is the fluid density.

Momentum equations: (j=1, 2, 3)

$$\frac{\partial}{\partial t}(\rho u_j) + \frac{\partial}{\partial x_i}(\rho u_i u_j) = -\frac{\partial p}{\partial x_j} + \frac{\partial \tau_{ij}}{\partial x_i} + \rho f_j \quad \text{.....(2)}$$

where p is the static pressure, τ_{ij} is the viscous stress tensor and f_j is the body force. For Newtonian fluids τ_{ij} can be expressed as:

$$\tau_{ij} = \mu\left(\frac{\partial u_i}{\partial x_j} + \frac{\partial u_j}{\partial x_i}\right) - \frac{2\mu}{3}\left[\frac{\partial u_k}{\partial x_k}\right]\delta_{ij} \quad \text{.....(3)}$$

where μ is the fluid dynamic viscosity and δ_{ij} is the Kronecker delta.

Energy Equation:

The equation for the conservation of energy can take several forms. The static enthalpy form of the energy equation can be expressed as:

$$\frac{\partial}{\partial t}(\rho h) + \frac{\partial}{\partial x_j}(\rho u_j h) = -\frac{\partial q_j}{\partial x_j} + \frac{\partial p}{\partial t} + u_j \frac{\partial p}{\partial x_j} + \tau_{ij}\frac{\partial u_i}{\partial x_j} - \frac{\partial}{\partial x_j}(J_{mj} h_m) \quad \text{.....(4)}$$

where J_{mj} is the total (concentration-driven + temperature-driven) diffusive mass flux for species m, h_m represents the enthalpy for species m, and q_j is the j-component of the heat flux. J_{mj}, h_m and h are given as:

$$J_{mj} = -\rho D \frac{\partial Y_m}{\partial X_j} \quad \text{.....(5)}$$

$$h_m = \int_{T_o}^{T} C_{P_m}(T)dT + h_{f_m}^o \quad \text{.....(6)}$$

$$h = \sum_{m=1}^{n} Y_m h_m \quad \text{.....(7)}$$

where D is the diffusion coefficient, C_p is the constant-pressure specific heat, and h_f^o is the enthalpy of formation at standard conditions (P_o=1 atm, T_o=298 K).

The Fourier's law is employed for the heat flux:

$$q_j'' = -K\frac{\partial T}{\partial x_j} \quad \text{.....(8)}$$

where K is the thermal conductivity.

Mixture Fractions:

$$\frac{\partial}{\partial t}(\rho f_k) + \frac{\partial}{\partial x_j}(\rho u_j f_k) = \frac{\partial}{\partial x_j}\left(D\frac{\partial f_k}{\partial x_j}\right) \quad \text{.....(9)}$$

where D is the diffusion coefficient, f_k is the mixture fraction for the k^{th} mixture.

Chemistry/Reaction Model

The reaction model used by CFD-ACE+ was the instantaneous chemistry model in which the reactants are assumed to react completely upon contact. The reaction rate is infinitely rapid and one reaction step is assumed. Two reactants, which are commonly referred to as "fuel" and "oxidizer", are involved. A surface "flame sheet" separates the two reactants (this assumption can be made only for nonpremixed flames). The mass fractions for this model are computed by first using Eq. 10 to obtain the composition that would occur without the reaction. The "unreacted" composition, denoted by the superscript "u", is given by

$$(Y_i)^u = \sum_{k=1}^{K} \xi_{ik} f_k \quad \text{.....(10)}$$

where ξ_{ik} is the mass fraction of the i^{th} species in the k^{th} mixture, Y_i is the mass fraction of the i^{th} species and f_k is the mixture fraction of the k^{th} mixture. The change in composition due to the instantaneous reaction is then added to the unreacted mass fractions, as described below.

A stoichiometrically correct reaction step needs to be specified. The mass of species i produced per unit mass of fuel consumed is

$$r_i = -\frac{\nu_i M_i}{\nu_f M_f} \quad \text{.....(11)}$$

where ν is the stoichiometric coefficient of the species in the overall reaction; positive for product species and negative for fuel and oxidizer. The instantaneous reaction mechanism consumes either all the fuel or all the oxidizer, whichever is limiting. The amount of fuel consumed is

$$\Delta Y_f = \min\left(\frac{(Y_f)^u}{-r_f}, \frac{(Y_{ox})^u}{-r_{ox}}\right) \quad \text{.....(12)}$$

The change in each species due to the reaction is proportional to the change in fuel, with the proportionality constant given by Eq. 11. The mass fraction of each species is then given by

$$Y_i = (Y_i)^u + r_i \Delta Y_f \quad \text{.....(13)}$$

The right-hand side of the above equation is only a function of the K mixture fractions. Therefore, K-1 transport equations were solved for the mixture fractions. These equations have no source terms due to chemical reactions (for more details see Qubbaj[22]).

In this analysis no chemistry model is introduced for the prediction of NO_x formation, and nitrogen is assumed to be chemically inert. NO_x is typically present in very low concentrations in the range of tens to hundreds of parts-per-million (ppm) and therefore has a negligible impact on the major physico-chemical process in combustion. Moreover, NO_x chemistry is orders of magnitude slower compared to the reaction rate of the fuel. NO_x formation is therefore not directly influenced by turbulent mixing; rather it is influenced by mean concentration levels of the primary constituents in the mixture. For this reason, NO_x related computations are typically done in a post-processing phase. Even without a NO_x model, often very useful qualitative information can be gained by studying various aspects of the numerical solution. For example, a high flame temperature and excess amounts of oxygen in the exhaust gases may be indicative of high NO_x emission levels.

D. RESULTS AND DISCUSSION

Figure 2 shows the radial temperature profiles for baseline, cascaded, air-swirling, and swirling-cascaded flames in the near burner region, which corresponds to an axial location

of x/d=4.63. This near burner region is of primary interest in this study since this is the area where most of the mixing and reactions take place. From the temperature profiles, the following observations can be made: (i) the off-axis peak exists in all cases, however, its radial location moves further inward in the cases of swirl and cascade and outward in the swirl-cascade; (ii) the peak temperature of the air-swirling and cascaded flames drop by 8% and 11%, respectively, from its baseline value, whereas that of the swirl-cascade increases by 8%; (iii) the swirl and cascade profiles are shifted inward towards the fuel-rich side of the flame, whereas the swirl-cascade one is shifted outward; (iv) the air-swirling and cascaded flames have significantly lower temperatures in the fuel-lean side of the flame, compared to the baseline case. However, it has higher valley temperatures in the fuel-rich side. The opposite trend is seen for the swirl-cascade.

The observed shift of the temperature profiles towards the fuel-rich side of the flame, in both the swirl and cascade cases, is a result of the air-swirling and venturi-cascade effects, respectively. The former produces a recirculation zone that sustains the entrainment process of the air stream into the fuel stream (Qubbaj et al.[1]), Whereas, the latter ejects the co-flow air stream into the core of the combustion zone by the effect of the venturi. Both effects lead to a rapid homogenization and better mixing rates of air with the unburned fuel of the mixture, and the consequent shift of the stoichiometric contour towards the center of the flame. This leaning process has two different effects on the fuel-lean and fuel-rich sides of the flame; the temperature of the latter increases while that of the former decreases. The valley temperature increase in the fuel-rich side of the swirling and cascaded flames is a result of higher oxygen availability, which pushes the mixture towards stoichiometry. On the other hand, the temperature decrease in the lean side is due to the excess air, which drives the mixture far away from stoichiometry. The higher peak temperature and outward shift of the swirl-cascade profiles indicate a poor mixing rates of air and fuel, and thereby counteracting the air-swirling and venturi effects seen earlier. The higher temperature would also suggest higher levels of NOx.

Figure 3 depicts the radial concentration profiles of CO_2 at the same conditions pertaining to the earlier temperature profiles. The existence of off-axis peaks, their radial locations, the shift of the profiles, the CO_2 concentrations in the fuel rich and fuel-lean sides, all follow the temperature profiles and similar explanations apply. This is reasonable, since

CO_2 is a direct combustion product, which depends primarily on temperature and stoichiometry of the flame.

Figure 4 shows the O_2 radial concentration profiles for the baseline, air-swirling, cascaded, and swirling-cascaded flames in the near-burner region. From these profiles the following can be observed: (i) the O_2 concentration starts with a zero value at the central axis and starts to build up in the radial outward direction until it attains its atmospheric value (~21%) near the outside boundary of the flame; (ii) O_2 concentration in the both air-swirling and cascaded flames build up faster and consequently attain the ambient value earlier than in the baseline and swirl-cascade cases; (iii) O_2 profiles in the air-swirling and cascaded flames are shifted inward, whereas that of the swirl-cascade is shifted outward. This observation is similar to that seen earlier for temperature and CO_2 profiles.

The zero O_2 concentration observed in the fuel-rich region is consistent with the absence of CO_2 values observed earlier in the same region. The faster build-up rates in the air-swirling and cascaded flames, compared to the baseline flame, is a clear indication of the higher rates of mixing with air provided by the air-swirling and venturi effects, respectively. This increase of O_2 is the direct cause of the temperature drop observed earlier. On the other hand, the lower build-up rate in the swirl-cascade case depicts poor mixing rates, thereby diminishing the swirling and venturi effects. The inward/outward shifts of the profiles have been noticed for the earlier temperature and CO_2 profiles too, and therefore, the same aforementioned explanation applies.

Figure 5 shows the radial profiles of the axial velocity component (U) for the baseline, cascaded, air-swirling, and swirl-cascaded flames in the near burner region. These profiles reveal that both air-swirling and cascaded flames have a lower centerline velocity and a wider profile than the baseline flame. The opposite trends are seen for the swirling-cascaded flame. The lower centerline velocity in the air-swirling and cascaded cases suggests a shorter flame produced by the swirl and venturi effects, respectively. However, when combined in the swirling-cascaded flame, the higher centerline velocity implies a longer flame.

In general, for a circular jet, the centerline velocity decreases and the jet becomes wider as the jet grows downstream due to the viscous shear and more air entrainment. Therefore, the lower centerline velocity and wider profiles observed for the air-swirling and cascaded

flames, compared to the baseline case, are indications of the rapid and faster growth of the gas jet flame. However, this interpenetration process is due not to shear but rather to the air-swirling and venturi-cascade effects, respectively. The former effect induces a recirculation zone that sustains the entrainment process of the outer air stream into the inner fuel stream, whereas, the latter inducts more of the co-flow air stream into the combustion zone. Both effects present the capability of an efficient mixing between the streams in the regions near the fuel outlet, therefore leading to a rapid homogenization of the combustible mixture and a shortening of the flame. The higher O_2 concentration and lower axial centerline velocity, observed in Figs. 4 and 5 for the swirl and cascade cases, compared to the baseline case, substantiate the last verdict for a shorter flame. However, the opposite trends predicted in the swirl-cascade case supports the earlier argument of a longer flame.

The shorter flame length and the consequent shorter residence time (assuming constant flame velocity), combined with the predicted lower temperatures in Fig. 2, are strong indicatives of Low NOx emission levels in the swirl and cascade cases. On the other hand, the opposite trends in the swirl-cascade case constitute a strong indication for a higher level of NOx.

Figure 6 presents the transverse profiles of the radial velocity component (V) at the same conditions. The general trend for the baseline profile is that the radial velocity is zero at the centerline, then it increases to attain a peak value in the fuel-rich region, beyond which it starts decreasing until it reaches a minimum (negative) value close to the stoichiometric contour, then it starts increasing again in the fuel-lean side of the flame to attain an asymptotic value near the flame edge. The positive velocities predicted close to centerline imply an outward velocity direction due to jet momentum. On the other hand, the negative velocities noticed farther from the centerline indicate an inward velocity direction. The swirl and cascade profiles reveal well-pronounced zones characterized by negative values of the velocity caused by the adverse pressure gradient induced by the intense swirl and venturi effects, respectively. Such a zone is less pronounced in the swirl-cascade case. Therefore, a dramatic increase in the inward radial velocities compared to the outward velocities is predicted for both swirl and cascade, compared to the baseline and swirl-cascade cases. The more negative radial velocities with the swirl and cascade cases indicate clearly the generation of an additional inward flow (towards the centerline of the jet) by the effects of

the swirl and venturis, respectively, thereby leading to the higher rates of mixing and its consequent impact on the combustion process. However, such effects are diminished for the swirl-cascade case.

The last verdict appears to be surprising, since an enhanced performance was initially expected by combining the optimal performance of both swirl and cascade burners in what thought to be “an enhanced swirl-cascade burner”. Nevertheless, the numerical results showed that the optimal configurations of the cascaded and swirling flames would not necessarily produce an improved performance when combined together in a “swirl-cascade burner”. The location of the recirculation zone with respect to the venturi must have played an important role. In other words, the swirling and venturi-cascading (at such conditions) have hindered each other’s influence. The non-linearity and complexity of the system accounts for such a result, and therefore, all possible combinations, i.e. swirl numbers (SN) versus venturi diameter ratios (D/d), need to be considered.

E. CONCLUSIONS

- The swirl and cascade burners simulations have revealed the following, compared to the baseline case:
  - An efficient fuel/air mixing in the primary reaction zone
  - A shorter flame length as indicated by lower centerline axial velocity and higher O_2 in-flame concentrations
  - Low NOx emission levels implied by moderate temperatures and less residence time of the flame.
- The swirl-cascade burner simulation has revealed the following, compared to the baseline case:
  - A poor fuel/air mixing in the primary reaction zone
  - A longer flame length as indicated by higher centerline axial velocity and lower O_2 in-flame concentrations
  - Higher NOx emission levels implied by higher temperatures and more residence time of the flame.
- The optimal configurations of the cascade and swirl burners have not produced an improved performance when combined together in a “swirl-cascade burner”.

- The non-linearity and complexity of the system accounts for such a result, and therefore, all possible combinations, i.e. swirl numbers (SN) versus venturi diameter ratios (D/d), need to be considered.
- The location of the recirculation zone with respect to the venturi must have played an important role in the performance of the swirl-cascade burner. Therefore, a stream function contours analysis is needed.

F. REFERENCES

[1]Bowman, Craig. T., 1992, "Control of Combustion-Generated Nitrogen Oxide Emissions: Technology Driven By Regulations," *Twenty-Fourth Symposium (International) on Combustion*, Combustion Institute, Pittsburgh, pp. 859-878.

[2]Gupta, A. K. and Lilley, D. G., 1985, Flow field Modeling and Diagnostics, Abacus Press, Kent, UK.

[3]Kamal, A., and Gollahalli, S. R., 1993, "Effects of Noncircular Fuel Nozzle on the Pollutant Emission Characteristics of Natural Gas Burner for Residential Furnaces," *Combustion, Modeling, Cofiring and NOx Control, ASME. FACT*. Vol.17, *pp*. 41-50.

[4]Papanikolau, N. and Wierzba, I., 1996, "Effect of Burner Geometry on the Blowout Limits of Jet Diffusion Flames in a Co-Flowing Air Stream," *Journal of Energy Resources Technology*, Vol. 118, pp. 134-139.

[5]Papanikolau, N., Wierzba, I., and Fergusson, B., 1997, "The Structure of Jet Diffusion Flames Issuing into Co-Flowing Air Stream," *Energy Week*, Pennwell publications, Houston, TX, Book V, pp. 222-228.

[6]Turns, S. R., 2000, An Introduction to Combustion: Concepts and Applications, 2nd Edition, *McGraw-Hill Inc.*, NY.

[7]Tomeczek, J., Goral, J. and Gradon, B., 1995, "Gas dynamics Abatement of NOx Emission from Industrial Natural Gas Jet Diffusion Flames," *Combustion Science and Technology*, Vol. 105, *pp.* 55-65.

[8]Cheng, T. S., Chao, Y. C., Wu, D. C., Yuan, T., Lu, C., Cheng, C., and Chang, J. M., 1998, "Effects of Fuel-air mixing on Flame Structures and NOx Emissions in Swirling Methane Jet Flames," *Twenty-Seventh Symposium (International) on Combustion*, University of Colorado at Boulder, Co, August 2-7.

[9]Qubbaj, Ala R. and Gollahalli, S. R., 1999, "Combustion Characteristics of Gas Jet Diffusion Flames Enveloped by a Cascade of Venturis," *Combustion Science and Technology Journal*, Vol. 143, pp. 1-23.

[10]Qubbaj, Ala R. and Gollahalli, S. R., 2000, ”Numerical Modeling of the Flow Field of a Burning Gas Jet in a Venturi-Cascade Burner,” *Energy Sources Technology Conference and Exhibition*, February 14-17, 2000, New Orleans, Louisiana, USA.

[11]Lyons, V. J., 1981,” Fuel-Air Nonuniformity Effect on Nitric Oxide Emissions,” AIAA J., *Progress in Energy and Combustion*, Vol. 20, No. 5, p. 660.

[12]Tangirala, V., Chen, R. H., and Driscoll, J. F., 1987, ”Effect of Heat Release and Swirl on the Recirculation within Swirl-Stabilization Flames,” *Combustion Science and Technology*, Vol. 51, pp. 75-95.

[13]Chen, R. H., and Driscoll, J. F., 1988, “The Rule of the Recirculation Vortex in Improving Fuel-Air Mixing within Swirling Flames,” *Twenty-Second Symposium (International) on Combustion*, Combustion Institute, Pittsburgh, pp. 531-440.

[14]Fric, T. F., 1993, ”Effects of Fuel-Air Unmixedness on NOx Emissions,” *Journal of Propulsion and Power*, Vol. 9, No. 5, p. 708.

[15]Villermaux, E., 1998, “ Mixing and Spray Formation in Coaxial Jets,” *Journal of Propulsion and Power*, Vol. 14, No. 5, pp. 807-817.

[16]Hillemans, R., Lenze, B. and Leuckel W., 1986, ”Flame Stabilization and Turbulent Exchange in Strongly Swirling Natural Gas Flames,” *Twenty-First Symposium (International) on Combustion*, Combustion Institute, Pittsburgh, p. 1445.

[17]Ala Qubbaj, S. R. Gollahalli and John Villarreal, 2002, "Numerical Modeling of a Turbulent Gas Jet Flame in a Swirling Air Stream," *ASME International Engineering Technology Conference on Energy/Combustion and Alternative Energy Symposium*, February 4-6, Houston, Texas, USA.

[18]Charles, R. E., Emdee, J. L., Muzio, L. J. and Samuelsen, G. S., 1986, ”The Effect of Inlet Conditions on the Performance and Flow field Structure of a Non-Premixed Swirl-Stabilized Distributed Reaction,” *Twenty-First Symposium (International) on Combustion*, Combustion Institute, Pittsburgh, pp. 1455-1461.

[19]Starner, S. H. and Bilger R. W., 1989, ”Further Velocity Measurements in a Turbulent Diffusion Flame with Moderate Swirl,” *Combustion Science and Technology*, Vol. 63, *pp.* 257-274.

[20]Shen, D., Most, J. M., Joulain, P. and Bachman, J. S., 1994, ”The Effect of Initial Condotonsfor Swirl Turbulent Diffusion Flame with a Straight-exit Burner. *Combustion Science and Technology*, Vol. 100, *pp.* 203-224.

[21]Van doormaal, J. P. and Dryer, F. L., 1984, “Enhancements of the SIMPLE Methods for Predicting Incompressible Fluid Flows,” *Numerical Heat Transfer*, Vol. 7, pp. 147-163.

[22]Qubbaj, A. R., 1998, “An Experimental and Numerical Study of Gas Jet Diffusion Flames Enveloped by a Cascade of Venturis,” *Ph.D. Dissertation*, School of Aerospace and Mechanical Engineering, The University of Oklahoma, Norman, Oklahoma.

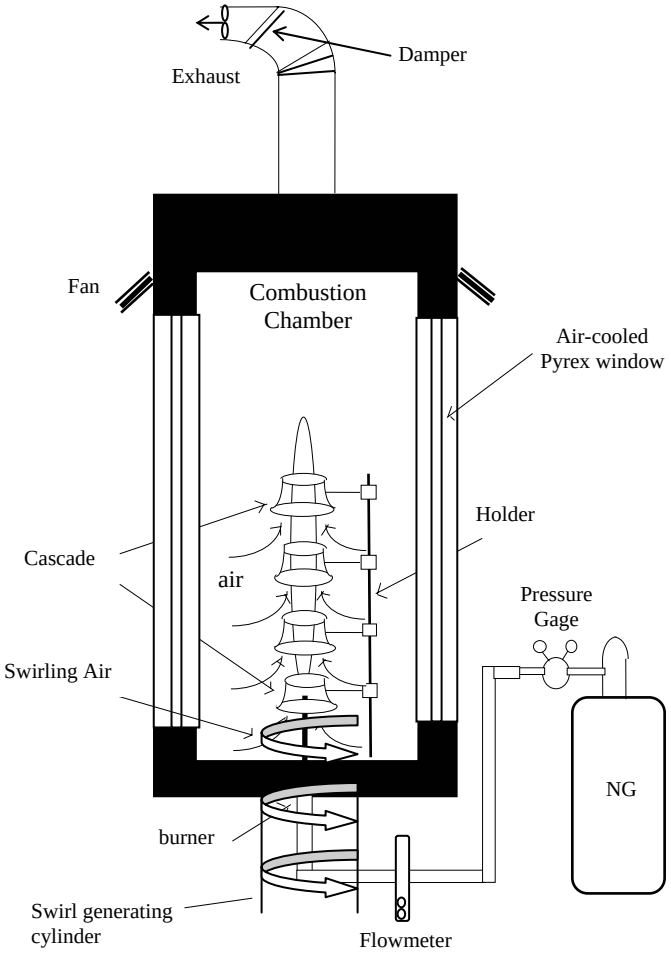

(A)

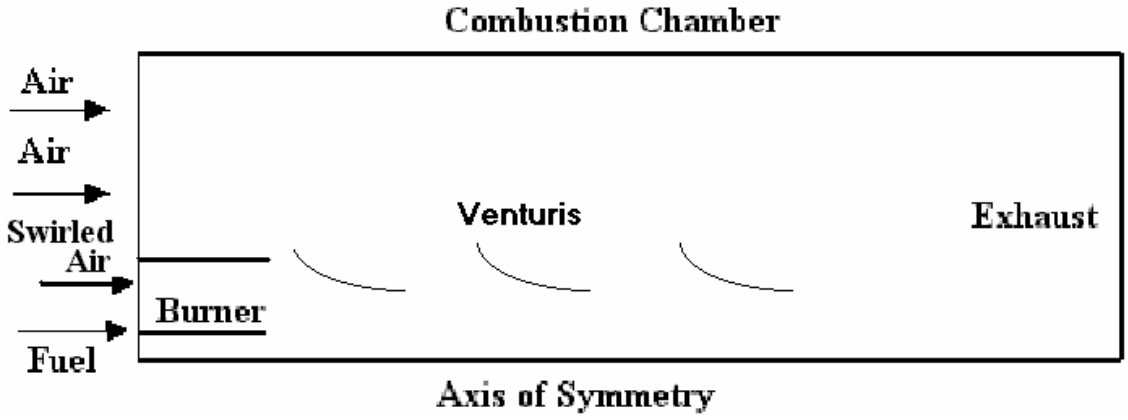

(B)

Figure 1: (a) Actual physical model (b) Simplified Problem geometry

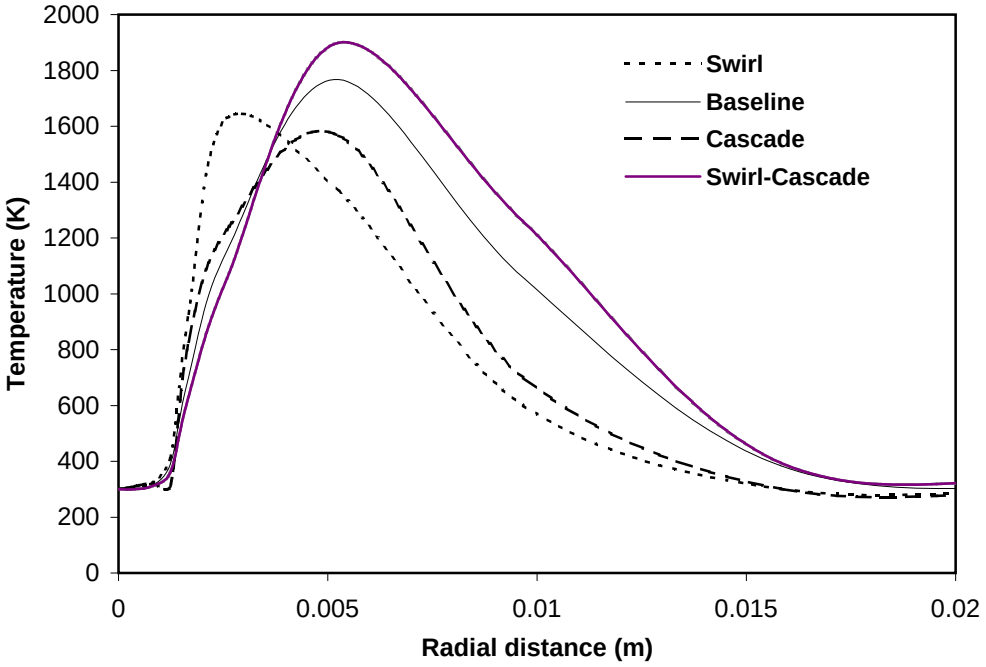

Fig. 2: Temperature Radial Profiles

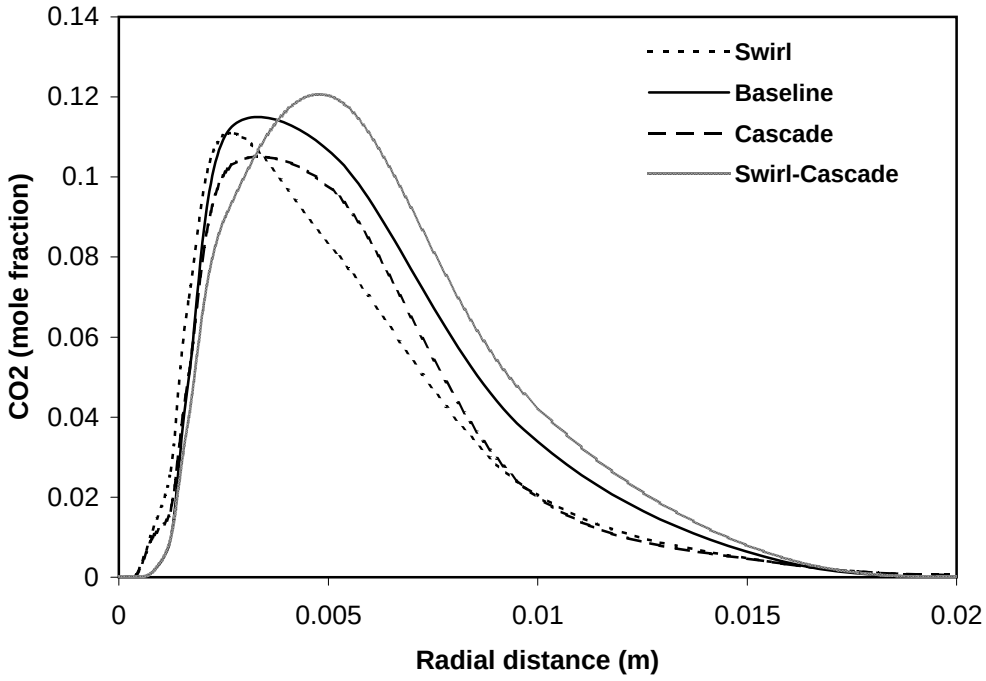

Fig. 3: Carbon Dioxide Radial Profiles

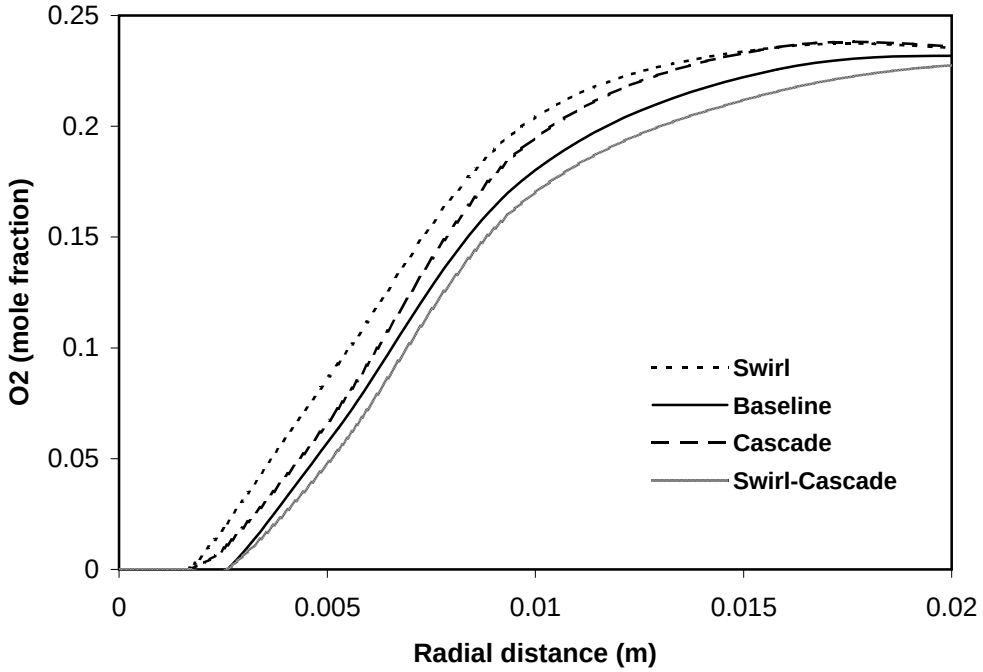

Fig. 4: Radial Oxygen Profiles

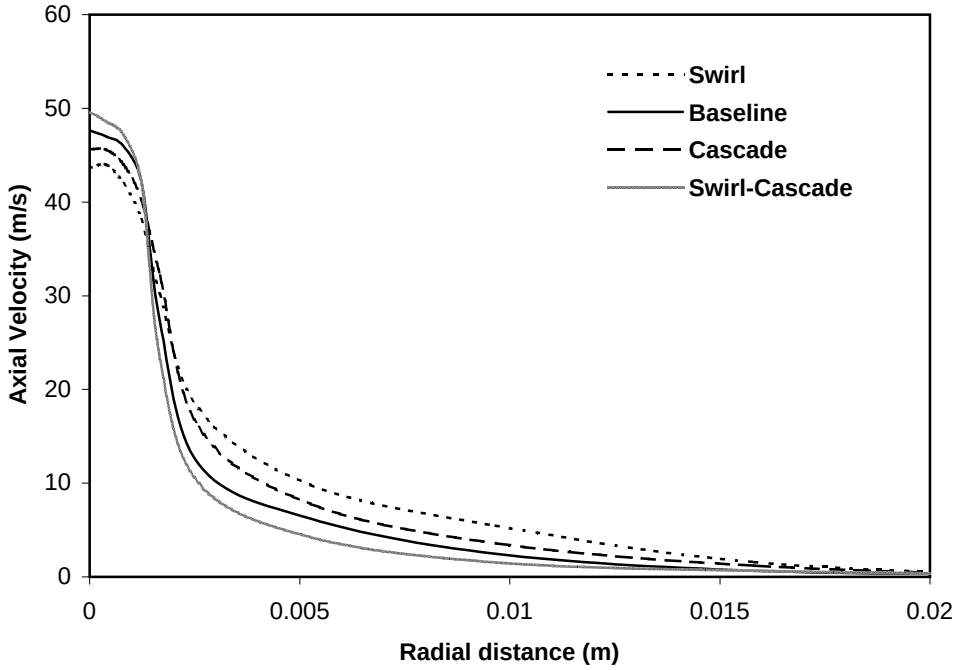

Fig. 5: Radial Profiles of Axial Velocity Component (U)

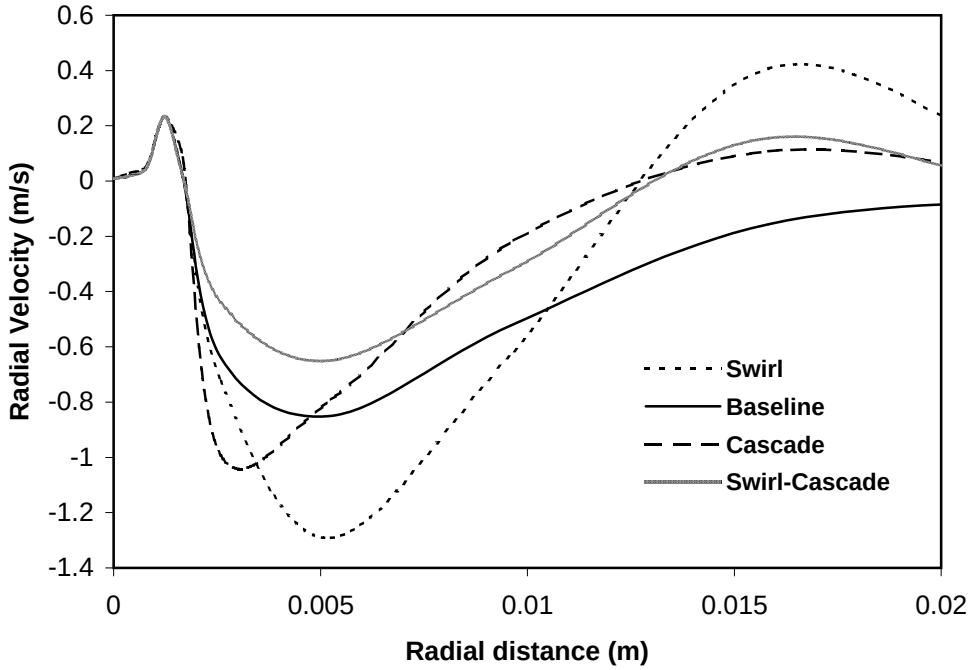

Fig. 6: Radial Profiles of Radial Velocity Component (V)